Journal of Engineering Research and Applied Science
Available at www.journaleras.com
Volume 11 (1), June 2022, pp 1982-1997
ISSN 2147-3471 © 2022

Petrographical, Geochemical and Petrological Characteristics of the Mafic Microgranular Enclaves in the Arpaköy (Kürtün/Gümüşhane) Granitoid

Abdullah Kaygusuz[1*], Zikrullah Samet Güloğlu[1]

[1]Gumushane University, Faculty of Engineering and Natural Science, Department of Geological Engineering, Gumushane, Turkey

Accepted 22 March 2022

Abstract
In this study, mineralogical-petrographical composition and whole-rock geochemical characteristics of the mafik microgranular enclaves (MMEs) in Arpaköy Granitoid in the Kürtün (Gümüşhane) area were determined, and the evolution and origin of the MMEs were investigated. The studied mafic microgranular enclaves (MMEs) are observed in Late Cretaceous Arpaköy Granitoid. Although these MMEs are finer grained and darker coloured than their host rocks, they aslo show similar mineralogic, petrographic and geochemical properties. The studied MMEs are gabroic diorite in composition, and composed of plagioclase (An_{65-41}), quartz, orthoclase, amphibole (Mg#=0.63-0.70), pyroxene and Fe-Ti oxides. Geochemically, the mafic microgranular enclaves (MMEs) has medium to high-K calc-alkaline and metaluminous characters and show similar geochemical characters to the host plutonic rocks. The MMEs are enriched in LILE and HREE, and show a concordant trend with the host rocks. Chondrite normalized REE patterns are concave shaped (La_N/Yb_N=7.11-11.57) and show negative Eu-anomalies (Eu_N/Eu^*=0.37-0.91). The crystallization temperatures calculated according to apatite and zircon are between 647 °C and 836 °C. When petrographic, geochemical and geothermometer studies are evaluated together, it is understood that the MMEs represent products of small masses during mixing/mingling processes of mafic parental magma of the host pluton in the crustal magma chamber.

Keywords: Arpaköy Granitoid, Eastern Pontides, Late Cretaceous, Mafic microgranular enclaves, Whole-rock geochemistry

1. Introduction

The Eastern Pontides (KD Turkey), located in the Alpin-Himalayan orogenic belt, is one of the important areas where volcanic and plutonic rocks are commonly observed [1–10]. There are many plutonic rocks with a wide range of age varying from Permo-Carboniferous to Eocene-Oligocene in the region (Figure 1). Especially Late Cretaceous aged ones from these plutonic rocks mostly include mafic microgranular enclaves (MMEs).

Mafic microgranular enclaves (MMEs) are related to the host plutonic rocks and they provide important information of their origins. Although there are many studies on MMEs (e.g [11–17], the studies on MMEs are limited in the Eastern Pontides [18–23].

Although the detailed studies related to the Arpaköy Granitoid made by [10], the studies on mineralogical-petrographic, micro chemical and whole-rock geochemical properties outside of the Tübitak Project Report [24] was not performed of the MMEs in the Arpaköy Granitoid.

*Corresponding author: abdullah.kaygusuz@gmail.com

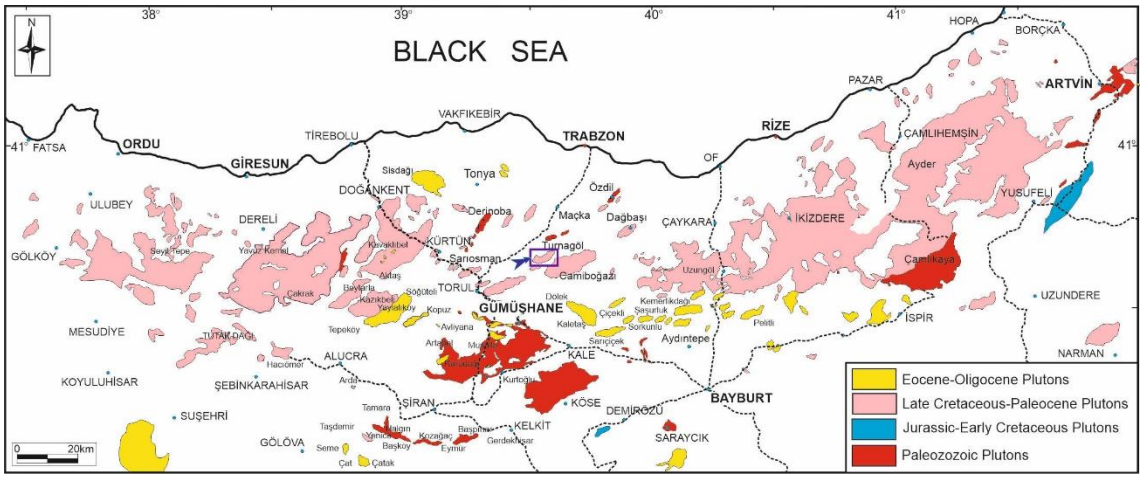

Figure 1. Geologic map showing distribution of Paleozoic to Eocene-Oligocene plutons in the Eastern Pontides (modified from [25,26])

In this study, the mineralogical-petrographic, micro chemical and whole-rock geochemical properties of the mafic microgranular enclaves (MMEs) in the Arpaköy Granitoid were determined, and the evolution and origin of the MMEs were investigated.

2. Material and Method

The thin sections of the MME samples collected from the field were prepared and detailed mineralogical-petrographic properties were examined under polarizing microscope. Modal analyses of the samples were made from the unaltered samples for determine the rock types of the samples. The modal mineralogy of five samples was determined by point counting with a swift automatic counter. Counting is generally carried out in the range of 0.4 mm, sometimes in the range of 0.2 mm. On each thin-section a total of 600–800 points were counted, and modes were normalized to 100%.

The major, trace and rare earth element (REE) analyzes of four mafic microgranular enclaves (MMEs) were made in analytical chemistry laboratories at ACME (Vancouver, Canada). The major and trace elements were analyzed by the ICP-AES method, while the rare earth elements were analyzed by the ICP-MS method. The loss on ignition (LOI) is calculated from the weight difference after the samples were burned in 1000 ^{O}C. Total Fe content is expressed of Fe_2O_3. Dedection limits range from 0.002 to 0.04 for the major oxides, from 0.01 to 8 ppm for trace elements and 0.01 to 0.3 ppm for REEs. The details of analysis technique are given by [10].

3. Findings and Discussion

3.1. Regional Geology and Stratigraphy

The Pre-Late Cretaceous units of the Eastern Pontides consist of Early Carboniferous metamorphic rocks [27], Late to Early Carboniferous Plutonic rocks [4,28–33], Early and Middle Jurassic volcano-sedimentary rocks [34–37], Mid to Late Jurassic plutonic rocks [38–40] and Late Jurassic to Early Cretaceous carbonates [41]. Late Cretaceous units, including plutonic rocks that hosted studied MMEs, are composed of plutonic, volcanic and sedimentary rocks [42–49]. Senozoic aged units consist of volcanic, plutonic and sedimentary rocks [2,50,59–61,51–58]. The youngest units in the region form Quaternary alluviums.

The study area is located in the northern zone of the Eastern Pontides. In the region, there are units in different ages and different lithologies from the Paleozoic to the end of the Tertiary (Figure 2). The oldest units in the study area form Paleozoic aged plutonic rocks. Liassic units which are consist of basalt, andesite and pyroclastic rocks are conformably overlies these units. Malm-Lower Cretaceous aged Berdiga Formation consisting of

sedimentary rocks are conformably overlies these Liassic units. Late Cretaceous Çatak Formation consisting of andesite, basalt and pyroclastic rocks lies above of these units and undertaken Late Cretaceous aged Kızılkaya Formation consisting of dacite and pyroclastic rocks. All these units were cut by Late Cretaceous aged Arpaköy Granitoid (Figure 2).

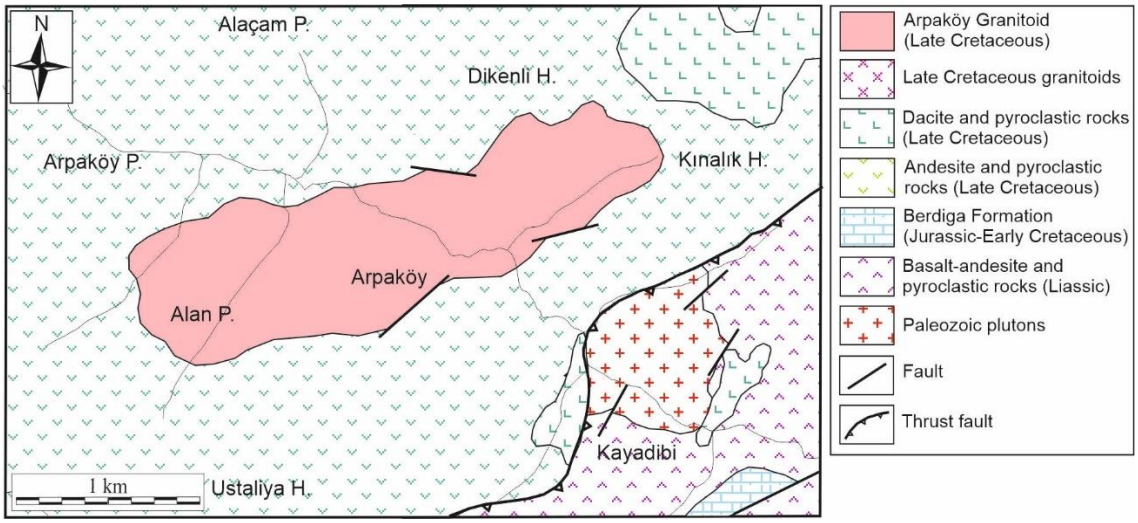

Figure 2. Geological map of the study area (modified from [10]

3.2. Field Observations

The Arpaköy Granitoid is approximately ellipse-shaped, and the long axis extends in the northeast-southwest direction (Figure 2). The Arpaköy Granitoid includes mafic microgranular anklav (MMA).

Enclaves in the Arpaköy Granitoid are called according to Didier and Barbarin (1991) classification. Enclaves with an oval shaped and fine-grained magmatic texture are called mafic microgranular enclaves (MMEs). Although the mafic microgranular enclaves observed in the Arpaköy Granitoid has made sharp contact with the host-rock, no metamorphism or metamorphism minerals were not found. They are angular or slightly ellipsoidal shaped and the dimensions range from 2 cm to 9 cm (Figure 3).

The elipsoidal shapes of the MMEs are due to their primitive physical properties and the ability to magmatic movement. All MMEs contain much more ferromagnesian minerals (e.g. hornblende), and the grain dimensions of the MMEs are smaller than the host-rocks (Figure 3).

Figure 3. Hand-space photograph of the MME in the Arpaköy Granitoid

3.3. Mineralogy and petrography

The modal analysis results of the five mafic microgranular enclave samples of the Arpaköy Granitoid are given in Table 1. The modal contents of the MMEs ranges from 68.9 to 71.2 for

*Corresponding author: abdullah.kaygusuz@gmail.com

plagioclase, from 1.1 to 3.8% for quartz, from 2.5 to 5.3 for orthoclase, from 13.3 to 14.8 for amphibole, from 4.6 to 7.5 for pyroxene and from 2.8 to 4.3 opaque minerals (Table 1). According to the results (Figure 4). of modal analysis, the mafic microgranular enclaves in the Arpaköy Granitoid are gabroic diorite in composition

Table 1. Modal analyzes of the MMEs in the Arpaköy Granitoid

Sample No	Rock name	Plagioclase	Quartz	Orthoclase	Amphibole	Pyroxene	Opaque minerals
T4a	Gbrdi	69.54	3.78	5.30	13.30	5.50	2.80
T3a	Gbrdi	69.95	3.15	4.20	13.85	4.60	4.30
M26a	Gbrdi	70.70	2.70	3.10	14.10	5.40	4.10
T2a	Gbrdi	68.85	2.45	4.85	14.35	6.10	3.60
T1a	Gbrdi	71.20	1.12	2.45	14.75	7.50	3.10
Gbrdi: Gabroic diorite							

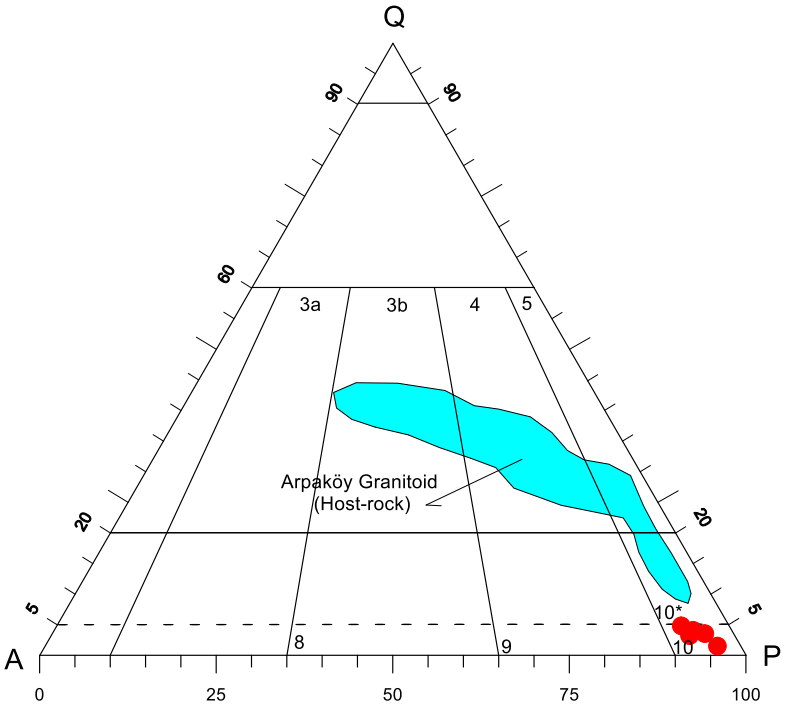

Figure 4. QAP classification diagram based on modal mineralogy of the MME samples in the Arpaköy Granitoid [62]

Gabroic diorite compound MMEs show fine-grained textures in microscopic examinations (Figure 5). The main minerals are composed of plagioclase, quartz, orthoclase, amphibole, pyroxene and opaque minerals. Accessory minerals are made up of apatite and zircon. The most common decomposition products are sericite, calcite, chlorite and clay minerals.

Plagioclases are small euhedral to subhedral crystals and are seen in all samples (Figure 5). They have police-twin and zoned structures. In the crystals of albite-twins, they are andesine (An_{47-36}) in composition. Some plagioclases are fractured and partially sericitized. K-feldispars are generally small anhedral crystals and are found at least. They fill out the other minerals with quartz. Quartz minerals are considerably observed, they fill in the gaps between the other minerals. Amphiboles are euhedral to subhedral small prismatic crystals. The most abundant mafic mineral in the sections and includes opaque minerals. Pyroxenes are euhedral to subhedral small crystals. They are augite in composition. In some sections, they are chloritization and calcititation. Apatites are seen as needle-like shapes and found as inclusions in plagioclase.

Zircons are observed as small euhedral prismatic crystals. Opaque minerals are found as euhedral and subhedral both large and small crystals.

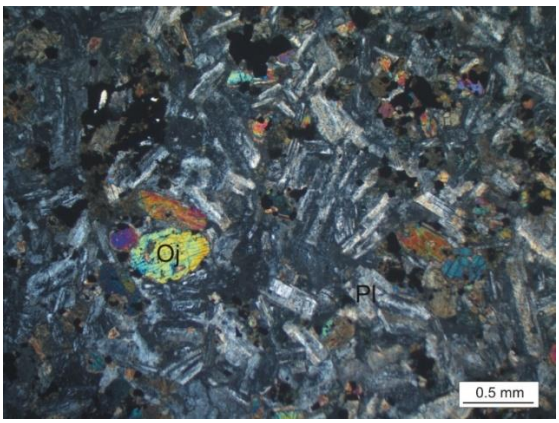

Figure 5. Fine-grained texture in mafic microgranular enclaves (crossed polars, Pl: plagioclase, Oj: augite)

3.4. Mineral Chemistry

3.4.1. Plagioclase

In all of the MMEs, the plagioclase minerals were observed. Microprob analysis results of plagioclase minerals in MME samples are given in Table 2. Considering the major element contents of the plagioclases in the MMEs, these values varying from 51.4 to 58.1% for SiO_2, 26.9 to 30.2% for Al_2O_3, 0.7 to 0.8% for FeO^T and 0.1 to 0.4% for K_2O (Table 2).

Table 2. Microprobe analysis results of the MMEs in the Arpaköy Granitoid

Sample No	T2a-05	T2a-06	T2a-20	T2a-21	T2a-16	T2a-17
SiO_2	51.35	52.15	54.25	55.35	57.04	58.12
Al_2O_3	30.18	29.16	28.05	27.89	27.26	26.87
FeO	0.78	0.72	0.69	0.71	0.70	0.68
CaO	13.18	12.25	10.91	9.85	8.84	8.46
Na_2O	3.82	4.12	5.18	5.67	6.13	6.45
K_2O	0.14	0.21	0.27	0.32	0.39	0.41
BaO	0.01	0.50	0.10	0.12	0.13	0.14
SrO	0.11	0.09	0.07	0.08	0.08	0.06
Total	99.58	99.20	99.52	99.99	100.56	101.19
Si	2.35	2.40	2.47	2.50	2.56	2.58
Al	1.63	1.58	1.51	1.49	1.44	1.41
$Fe^{(ii)}$	0.03	0.03	0.03	0.03	0.03	0.03
Ca	0.65	0.60	0.53	0.48	0.42	0.40
Na	0.34	0.37	0.46	0.50	0.53	0.56
K	0.01	0.01	0.02	0.02	0.02	0.02
Ba	0.00	0.01	0.00	0.00	0.00	0.00
Sr	0.00	0.00	0.00	0.00	0.00	0.00
An	65.05	61.39	52.93	48.07	43.35	41.03
Ab	34.11	37.36	45.49	50.07	54.39	56.60
Or	0.85	1.25	1.58	1.86	2.26	2.37
The formula has been calculated over 8 oxygen						

According to the results of the microprobe analysis, the compositions of the plagioclases observed of the MMEs in the Arpaköy Granitoid are An_{65-41}, similar to the host-rocks (Figure 6).

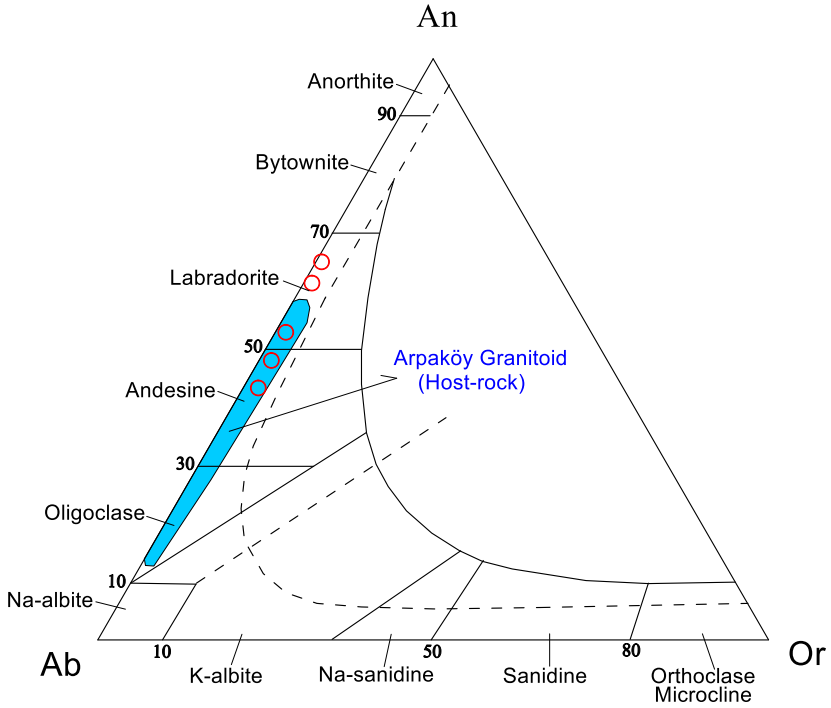

Figure 6. An-Ab-Or classification diagram [63] of the MMEs in the Arpaköy Granitoid

3.4.2. Amphibole

Amphiboles are observed in an important part of the mafic microgranular enclaves in the Arpaköy Granitoid. Microprob analysis values for amphiboles are given in Table 3. Considering the major element contents of the amphiboles in the MMEs, these values varying from 5.5 to 7.7% for Al_2O_3, 47.3 to 50.4% for SiO_2 and 0.6 to 0.7% for $Mg/(Mg+Fe^{+2})$ (Table 3). These values are similar to the host-rocks.

Table 3. Microprob analysis results of amphiboles of the MMEs in the Arpaköy Granitoid

Sample No	T2a-33	T2a-33	T2a-20	T2a-32	T2a-19	T2a-33
SiO_2	47.33	47.86	48.63	49.01	49.26	50.35
TiO_2	1.87	1.62	1.23	1.45	1.07	1.25
Al_2O_3	7.71	7.15	6.14	6.21	5.50	5.46
FeO	11.87	12.25	14.97	12.47	14.59	13.95
MnO	0.30	0.35	0.49	0.29	0.50	0.55
MgO	15.47	15.13	14.08	15.43	14.70	14.45
CaO	11.38	11.25	11.08	11.34	10.95	10.46
Na_2O	1.27	1.25	1.23	1.23	0.91	0.76
K_2O	0.53	0.51	0.49	0.39	0.37	0.32
Total	97.73	97.37	98.33	97.81	97.85	97.55
Si	6.76	6.87	6.97	6.99	7.03	7.16
Ti	0.20	0.17	0.13	0.16	0.12	0.13
Al^4	1.17	1.06	0.94	0.94	0.84	0.71
Al^6	0.14	0.16	0.11	0.12	0.11	0.23
Fe^{+2}	0.91	1.01	1.21	1.05	0.88	0.83
Fe^{+3}	0.51	0.46	0.59	0.44	0.86	0.83

Mn	0.04	0.04	0.06	0.03	0.06	0.07
Mg	3.29	3.24	3.01	3.28	3.13	3.06
Ca	1.74	1.73	1.70	1.73	1.67	1.59
Na	0.70	0.70	0.68	0.68	0.51	0.42
K	0.10	0.09	0.09	0.07	0.07	0.06
Mg/(Mg+Fe)	0.70	0.69	0.63	0.69	0.64	0.65
The formula has been calculated over 23 oxygen						

According to the results of the microprob analysis of amphiboles, the amphibols of the studied MMEs are magnesium hornblend in composition (Figure 7). They have similar composition with host-rocks (Figure 7).

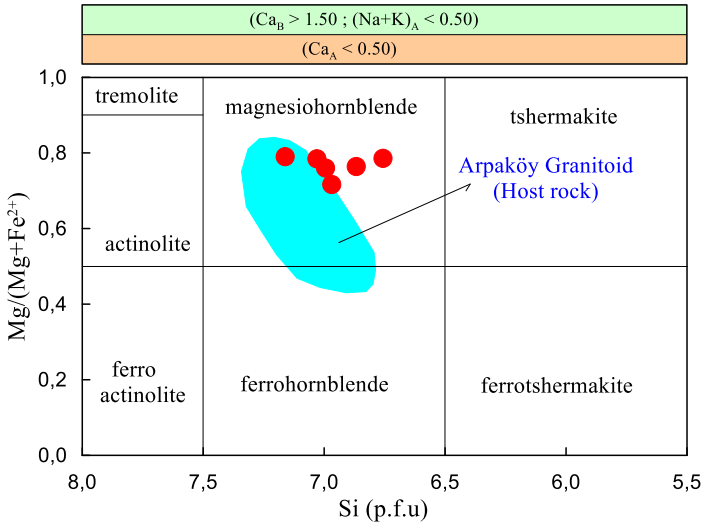

Figure 7. Composition of amphiboles [64]

3.5. Whole-rock geochemistry

Major and trace element analysis results of five mafic microgranular enclaves (MMEs) are given in Table 4, and rare earth element analysis are given in Table 5.

While SiO_2 values of the MMEs vary between 53.1 and 54.8%, MgO content varies between 2.4 and 3.7% (Table 4). K_2O/Na_2O ratios of the samples are less than 1 and are between 0.04 and 0.1. A/CNK values are between 0.86 and 0.89, and magnesium numbers (Mg#) are between 43 and 47 (Table 4). Compared to the host-rocks, they have higher MgO, FeO_3^T and CaO content and lower SiO_2 and K_2O content than host-rocks.

Table 4. Major (%) and trace (ppm) element analysis of the MMEs in Arpaköy Granitoid

Sample No	T1a	T2a	M26a	T3a	T4a
Rock Types	gbrdi	gbrdi	gbrdi	gbrdi	gbrdi
SiO_2	53.14	53.62	54.07	54.35	54.78
TiO_2	0.81	0.79	0.78	0.76	0.75
Al_2O_3	19.46	19.64	19.60	19.35	19.12
Fe_2O_3	8.98	8.82	8.78	7.56	7.23
MnO	0.21	0.19	0.18	0.16	0.17
MgO	3.65	3.12	3.05	2.75	2.43
CaO	9.44	9.38	9.33	9.18	9.12
Na_2O	2.85	2.92	3.00	3.15	3.28
K_2O	0.12	0.16	0.28	0.25	0.32
P_2O_5	0.22	0.20	0.19	0.16	0.17

LOI	0.80	0.80	0.70	2.00	2.30
Total	99.68	99.64	99.96	99.67	99.67
Ni	2.70	2.50	2.40	2.50	2.30
V	165.00	153.00	149.00	132.00	144.00
Cu	43.00	45.00	46.60	48.00	47.60
Pb	1.10	1.20	1.40	1.30	1.60
Zn	14.00	16.00	17.00	19.00	18.00
W	5.40	5.20	5.10	4.90	5.10
Rb	1.30	1.20	1.40	1.90	1.70
Ba	38.00	42.00	48.00	54.00	52.00
Sr	324.00	312.00	304.80	307.00	301.00
Ta	0.10	0.20	0.30	0.20	0.50
Nb	3.00	3.10	3.20	3.10	3.40
Hf	1.90	1.90	1.80	1.60	1.70
Zr	48.20	47.90	47.70	47.40	47.60
Y	14.50	14.40	14.30	14.10	14.20
Th	1.30	1.80	1.70	2.20	2.60
U	0.50	0.60	0.70	0.50	0.80
Ga	17.50	17.70	17.90	18.10	18.00
K_2O/Na_2O	0.04	0.05	0.09	0.08	0.10
Mg #	47.22	43.78	43.33	44.47	42.53
A /CNK (ASI)	0.89	0.89	0.88	0.87	0.86
$Fe_2O_3^T$ is total iron as Fe_2O_3, LOI is loss on ignition, Mg# (mg-number) = molar 100xMgO/(MgO+ $Fe_2O_3^T$), ASI (A/CNK) = molarAl_2O_3/(CaO+Na_2O+K_2O), gbrdi: gabroic diorite					

Table 5. Rare earth element (ppm) analysis of the MMEs in Arpaköy Granitoid.

Sample No	T1a	T2a	M26a	T3a	T4a
Rock Types	gbrdi	gbrdi	gbrdi	gbrdi	gbrdi
La	3.90	4.10	4.20	4.40	4.30
Ce	11.10	11.20	11.50	11.40	11.60
Pr	1.15	1.17	1.19	1.21	1.20
Nd	6.10	6.30	6.40	6.30	6.50
Sm	1.58	1.62	1.68	1.72	1.69
Eu	0.58	0.61	0.63	0.62	0.64
Gd	1.65	1.67	1.68	1.71	1.69
Tb	0.35	0.37	0.36	0.38	0.40
Dy	3.06	3.08	3.07	3.09	3.11
Ho	0.51	0.52	0.51	0.53	0.54
Er	1.47	1.49	1.48	1.51	1.54
Tm	0.28	0.32	0.31	0.35	0.34
Yb	2.06	2.08	2.07	2.09	2.08
Lu	0.33	0.35	0.34	0.35	0.37
(La/Lu)n	1.22	1.21	1.28	1.30	1.20
(La/Sm)n	1.55	1.59	1.57	1.61	1.60
(Gd/Lu)n	0.62	0.59	0.61	0.61	0.57
(La/Yb)n	1.28	1.33	1.37	1.42	1.40
(Tb/Yb)n	2.70	3.70	3.51	4.50	5.34

(Eu/Eu*)n	1.09	1.12	1.13	1.09	1.15
Eu* = (Sm+Gd)n/2					

In the (Na_2O+K_2O) vs. SiO_2 diagram, the MMEs are composed of gabbroic diorite (Figure 8a).

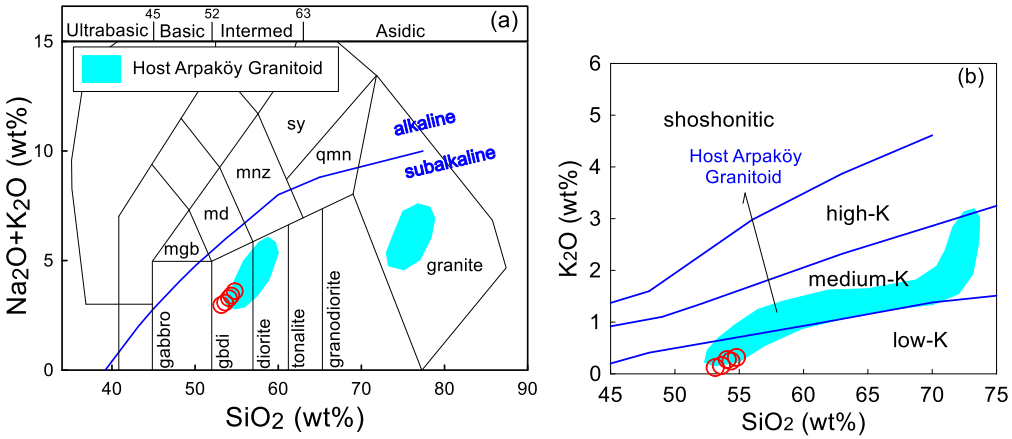

Figure 8. The samples belonging to the MMEs in the Arpaköy Granitoid, (a) (Na_2O+K_2O) vs. SiO_2 diagram [65], (b) K_2O vs. SiO_2 diagram [66]

In the K_2O vs. SiO_2 diagram, subalkaline samples forming the MMEs present a low potassium calc-alkaline composition (Figure 8b). They have lower K_2O values compared to the host-rocks (Figure 8b).

In the SiO_2 vs. ASI (molar $Al_2O_3/(CaO+Na_2O+K_2O)$ diagram, MMEs are located in the metalluminous field, and the host-rocks are in the metalluminous-peraluminous fields (Figure 9a). In the Nb vs. 10000Ga/Al diagram, the MMEs and host-rocks are located in the I-type area (Figure 9b).

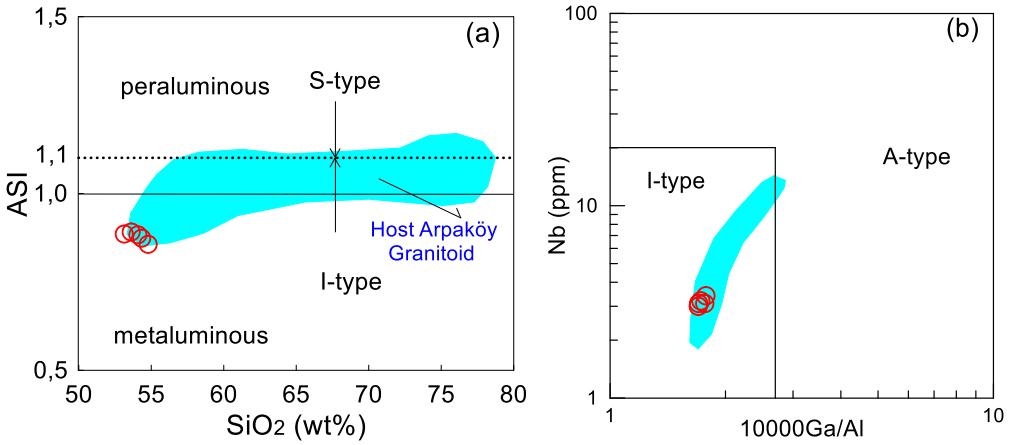

Figure 9. Rock samples from the MMEs, (a) SiO_2 vs. ASI diagram (fields: [67,68], (b) Nb vs. 10000Ga/La [69] diagram

In the trace element variation diagram normalized to the primitive mantle [70] (Figure 10a), the MMEs show a similar distribution with the host-rocks. The samples of the MMEs and Arpaköy Granitoid show an enrichment. However, this enrichment is less in MMEs than host-rocks. A negative anomaly is evident in Nb and Ta (Figure 10a).

In the chondrite-normalized [71] rare earth element diagrams (Figure 10b), MMEs are less enriched than the host-rocks. $(La/Lu)_N$ values of the MMEs are between 1.20 and 1.30, $(La/Sm)_N$ values are between 1.55 and 1.61, and $(Gd/Lu)_N$ values are between 0.57 and 0.62 (Table 5, Figure 10b). Eu_N values of the samples are greater than 1 (1.09-1.15) and show positive Eu_N (Eu/Eu*) anamolies. They present a distribution similar to the host-rocks (Figure 10b).

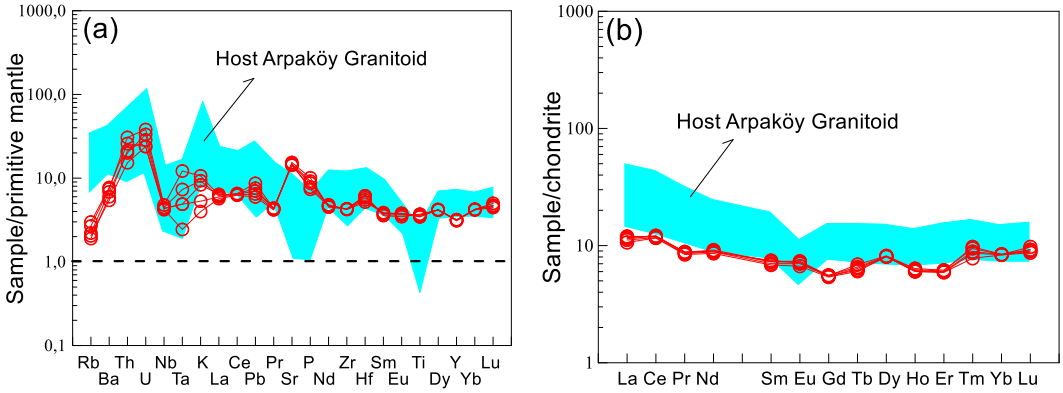

Figure 10. The MMEs in the Arpakoy Granitoid (a) Primitive mantle normalized trace element patterns [70], (b) Chondrite-normalised trace element patterns [71]

3.6. Intensive parameters

3.6.1. Amphibole-plagioclase geobarometer

$Al^{(T)}$ content of amphiboles crystallising from granitoid magmas is known to be an indicator of pressure and pressure calculations are used with the aid of a variety of calibrations. In granitoid rocks, the $Al^{(T)}$ content of amphiboles are used with the calibrations used for pressure estimation given below. The details about the calibrations are given by [61].

P (kbar)= 4.76 $Al^{(T)}$ - 3.01 [72]
P (kbar)= 5.03 $Al^{(T)}$ - 3.92 [73]
P (kbar)= 5.64 $Al^{(T)}$ - 4.76 [74]

The pressures calculated on the basis of the aluminum-horblende geobarometer in amphiboles are given in Table 6. Calculated pressure values of the MMEs vary between 0.4 and 3.2 kbar.

Table 6. The minimum, maximum and average pressure values of the MMEs.

Sample (n=6)	Si	Al (pfu)	Pl (Ab)	P (kbar)[1]	P (kbar)[2]	P (kbar)[3]
Min	6.83	0.92	22.28	0.68	0.40	1.35
Max	7.29	1.30	68.93	2.60	2.56	3.16
Avg	7.06	1.07	49.01	1.47	1.28	2.09
[(1)] Calculated from the calibration of [73] [(2)] Calculated from the calibration of [74] [(3)] Calculated from the calibration of [72]						

3.6.2. Amphibole-plagioclase geothermometer

The amphibole-plagioclase thermometer recommended by [75] was used to estimate the crystallisation temperature of the magmas. This thermometer calculates temperature with the formula of T= 0.667 P - 48.98 + *Y*/- 0.0429 - 0.008314 LnK. The details about the calibrations are given by [61].

In the samples of the studied MMEs, the above calibration was used for temperature predictions, and it was determined that the temperature values were similar to each other. Calculated crystallization temperatures of the MMEs vary between 737 and 801 ºC (Table 7).

*Corresponding author: abdullah.kaygusuz@gmail.com

Table 7. The minimum, maximum and average temperature values in the MMEs

Sample (n=6)	Si	$Al^{(T)}$	Ab	T °C
Min	6.83	0.92	22.28	737
Max	7.29	1.30	68.93	801
Avg	7.06	1.07	49.01	773
Calculated from the calibration of [75]				

3.6.3. Zircon and apatite geothermometer

Apatite and zircon saturation temperatures [76–78] are calculated from the whole-rock geochemical analyzes of rock samples. Temperature values vary depending on the maximum or minimum temperature of the intruding magma and whether the melt was saturated or undersaturated by these components. While the Zr abundances in the MME samples in the Arpaköy Granitoid result in zircon saturation temperatures of 645-647 ºC, the calculated apatite saturation temperatures vary between 764 and 783 ºC (Table 8).

Table 8. Minimum, maximum and average temperature values from the MMEs

Sample (n=5)	T °C (Zircon)	T °C (Apatite)
Min	645	764
Mak	647	783
Avg	646	776

3.6.4. The origin of the MMEs in the Arpaköy Granitoid

There are many arguments about magmatic vs. nonmagmatic origin of the MMEs. The studied MMEs display igneous textures (Figure 3a), indicating that they have a magmatic origin. This observation excludes the possibility that the MMEs are xenoliths or restites, because xenoliths or restites typically have metamorphic or residual sedimentary fabric [79]. Also, restite enclaves are identified with clear metamorphic textures and Al-minerals (garnet, sillmanite, etc.) and dominently enclosed in S-type granitoids. The MMEs of the studied plutons can also not be explained as cumulates because of the absence of a cumulate texture [14]. Petrographical observations and geochemical features (i.e., quenched margins, acicular apatites within the MMEs), lower ASI values of the MMEs (0.86 to 0.89), and strong correlations between major and trace elements, are indicative of magma mixing/mingling. Thus, the MMEs represent products of small masses during mixing/mingling processes of mafic parental magma of the host granitoid in the crustal magma chamber.

4. Conclusions

1. The studied mafic magmatic enclaves (MMEs) are located within the Late Cretaceous aged Arpaköy Granitoid.
2. The studied MMEs are gabbroic diorite in composition and show similar mineralogical and petrographic properties with their host-rocks. However, they are distinguished from them by their finer-grained texture and higher content of mafic minerals.
3. The studied MMEs mainly consist of plagioclase, quartz, orthoclase, amphibole, pyroxene and opaque minerals.
4. SiO_2 contents of the studied MMEs are between 53 and 55wt.%, and they have lower SiO_2 values than host-rocks.
5. The studied MMEs have I-type, low-K calc-alkaline and metalluminous characters.

6. The crystallization temperatures of the studied MMEs, calculated according to apatite-zircon geothermometry, vary between 645 and 783 ºC.
7. The crystallization temperatures of the studied MMEs, calculated according to the amphibole-plagioclase geothermometer, are between 737 and 801 °C.
8. The crystallization pressures of the studied MMEs, calculated according to the amphibole-plagioclase geobarometer, are between 0.4 and 3.2 kbar.
9. The studied mafic magmatic enclaves (MMEs) have similar geochemical properties with the host-rock and are represent products of small masses during mixing/mingling processes of mafic parental magma of the host granitoid.

Acknowledgment

This work was partially supported by the TUBITAK project number 109Y052. We appreciate to the editor and anonymous referees that contribute to the improvement of the manuscript.

References

[1] Akaryalı E. Geochemical, fluid inclusion and isotopic (O, H and S) constraints on the origin of Pb–Zn±Au vein-type mineralizations in the Eastern Pontides Orogenic Belt (NE Turkey). Ore Geol Rev 2016; 74:1–14.

[2] Arslan M, Temizel İ, Abdioğlu E, Kolaylı H, Yücel C, Boztuğ D, Şen C. 40Ar–39Ar dating, whole-rock and Sr–Nd–Pb isotope geochemistry of post-collisional Eocene volcanic rocks in the southern part of the Eastern Pontides (NE Turkey): implications for magma evolution in extension-induced origin. Contrib to Mineral Petrol 2013; 166:113–142.

[3] Dokuz A, Uysal I, Siebel W, Turan M, Duncan R, Akçay M. Post-collisional adakitic volcanism in the eastern part of the Sakarya Zone, Turkey: Evidence for slab and crustal melting. Contrib to Mineral Petrol 2013; 166:1443–1468.

[4] Kaygusuz A, Aydınçakır E, Yücel C, Atay HE. Petrographic and geochemical characteristics of carboniferous plutonic rocks around Erenkaya (Gümüşhane, NE Turkey). J Eng Res Appl Sci 2021; 10:1774–1778.

[5] Vural A, Kaygusuz A. Geochronology, petrogenesis and tectonic importance of Eocene I-type magmatism in the Eastern Pontides, NE Turkey. Arab J Geosci 2021; 14.

[6] Aydınçakır E, Yücel C, Ruffet G, Gücer MA, Akaryalı E, Kaygusuz A. Petrogenesis of post-collisional Middle Eocene volcanism in the Eastern Pontides (NE, Turkey): Insights from geochemistry, whole-rock Sr-Nd-Pb isotopes, zircon U-Pb and 40Ar-39Ar geochronology. Geochemistry 2022:125871.

[7] Yücel C, Arslan M, Temizel I, Abdioğlu E. Volcanic facies and mineral chemistry of Tertiary volcanics in the northern part of the Eastern Pontides, northeast Turkey: Implications for pre-eruptive crystallization conditions and magma chamber processes. Mineral Petrol 2014; 108:439–467.

[8] Kaygusuz A, Siebel W, Şen C, Satir M. Petrochemistry and petrology of I-type granitoids in an arc setting: The composite Torul pluton, Eastern Pontides, NE Turkey. Int J Earth Sci 2008; 97:739–764.

[9] Sipahi F, Saydam Eker Ç, Akpınar İ, Gücer MA, Vural A, Kaygusuz A, Aydurmuş T. Eocene magmatism and associated Fe-Cu mineralization in northeastern Turkey: a case study of the Karadağ skarn. Int Geol Rev 2021:1–26.

[10] Kaygusuz A, Arslan M, Temizel İ, Yücel C, Aydınçakır E. U–Pb zircon ages and petrogenesis of the Late Cretaceous I-type granitoids in arc setting, Eastern Pontides, NE Turkey. J African Earth Sci 2021; 174:104040.

[11] Vernon RH. Microgranitoid enclaves in granites-globules of hybrid magma quenched in a plutonic environment. Nature 1984; 309:438–439.

[12] Barbarin B, Didier J. Genesis and evolution of mafic microgranular enclaves through various types of interaction between coexisting felsic and mafic magmas. Earth Environ Sci Trans R Soc Edinburgh 1992; 83:145–153.

[13] Kadioğlu YK, Güleç N. Types and genesis of the enclaves in Central Anatolian granitoids. Geol J 1999; 34:243–256.

[14] Barbarin B. Mafic magmatic enclaves and mafic rocks associated with some granitoids of the central Sierra Nevada batholith,

California: Nature, origin, and relations with the hosts. Lithos 2005; 80:155–177.

[15] Chen S, Niu Y, Sun W, Zhang Y, Li J, Guo P, Sun P. On the origin of mafic magmatic enclaves (MMEs) in syn-collisional granitoids: evidence from the Baojishan pluton in the North Qilian Orogen, China. Mineral Petrol 2015; 109:577–596.

[16] Ilbeyli N, Pearce JA. Petrogenesis of igneous enclaves in plutonic rocks of the central anatolian crystalline complex, Turkey. Int Geol Rev 2005; 47:1011–1034.

[17] Kocak K. Hybridization of mafic microgranular enclaves: Mineral and whole-rock chemistry evidence from the Karamadazi Granitoid, Central Turkey. Int J Earth Sci 2006; 95:587–607.

[18] Karslı O, Chen B, Uysal I, Aydın F, Wijbrans JR, Kandemir R. Elemental and Sr–Nd–Pb isotopic geochemistry of the most recent Quaternary volcanism in the Erzincan Basin, Eastern Turkey: framework for the evaluation of basalt–lower crust interaction. Lithos 2008; 106:55–70.

[19] Kaygusuz A, Aydınçakır E. Mineralogy, whole-rock and Sr-Nd isotope geochemistry of mafic microgranular enclaves in Cretaceous Dagbasi granitoids, Eastern Pontides, NE Turkey: Evidence of magma mixing, mingling and chemical equilibration. Chemie Der Erde 2009; 69:247–277.

[20] Kaygusuz A, Arslan M, Siebel W, Sipahi F, Ilbeyli N, Temizel İ. LA-ICP MS zircon dating, whole-rock and Sr-Nd-Pb-O isotope geochemistry of the Camiboğazi pluton, Eastern Pontides, NE Turkey: Implications for lithospheric mantle and lower crustal sources in arc-related I-type magmatism. Lithos 2014; 192–195:271–290.

[21] Temizel I. Petrochemical evidence of magma mingling and mixing in the Tertiary monzogabbroic stocks around the Bafra (Samsun) area in Turkey: Implications of coeval mafic and felsic magma interactions. Mineral Petrol 2014; 108:353–370.

[22] Özdamar Ş, Zou H, Billor MZ, Hames WE. Petrogenesis of mafic microgranular enclaves (MMEs) in the oligocene-miocene granitoid plutons from northwest Anatolia, Turkey. Geochemistry 2021; 81.

[23] Yilmaz Şahin S. Geochemistry of mafic microgranular enclaves in the Tamdere Quartz Monzonite, south of Dereli/Giresun, Eastern Pontides, Turkey. Chemie Der Erde 2008; 68:81–92.

[24] Kaygusuz A, Arsan M, İlbeyli N, Sipahi F. Doğu Pontid Kuzey Zonu ve Kuzey-Güney Zon Geçişinde Yüzeylenen Kretase-Paleosen Yaşlı Granitoyidik Sokulumların Petrokimyası, Sr-Nd-Pb-O izotop Jeokimyası, Jeokronolojisi ve Jeodinamik Gelişimi. Tübitak Projesi Sonuç Raporu, Proje No 109Y052, 2012:1–199.

[25] Güven İH. Doğu Pontidlerin 1:25000 ölçekli kompilasyonu. MTA Genel Müdürlüğü 1993.

[26] Kaygusuz A, Yücel C, Arslan M, Temizel İ, Yi K, Jeong YJ, Siebel W, Sipahi F. Eocene I-type magmatism in the Eastern Pontides, NE Turkey: insights into magma genesis and magma-tectonic evolution from whole-rock geochemistry, geochronology and isotope systematics. Int Geol Rev 2020; 62:1406–1432.

[27] Topuz G, Altherr R, Kalt A, Satir M, Werner O, Schwarz WH. Aluminous granulites from the Pulur complex, NE Turkey: A case of partial melting, efficient melt extraction and crystallisation. Lithos 2004; 72:183–207.

[28] Topuz G, Altherr R, Siebel W, Schwarz WH, Zack T, Hasözbek A, Barth M, Satir M, Şen C. Carboniferous high-potassium I-type granitoid magmatism in the Eastern Pontides: The Gümüşhane pluton (NE Turkey). Lithos 2010; 116:92–110.

[29] Dokuz A. A slab detachment and delamination model for the generation of Carboniferous high-potassium I-type magmatism in the Eastern Pontides, NE Turkey: The Köse composite pluton. Gondwana Res 2011; 19:926–944.

[30] Vural A, Kaygusuz A. Petrology of the paleozoic plutons in Eastern pontides: artabel pluton (Gümüşhane, NE Turkey). J Eng Res Appl Sci 2019; 8:1216–1228.

[31] Karslı O, Dokuz A, Kandemir R. Subduction-related Late Carboniferous to Early Permian Magmatism in the Eastern Pontides, the Camlik and Casurluk plutons: Insights from geochemistry, whole-rock Sr–Nd and in situ zircon Lu–Hf isotopes, and U–Pb geochronology. Lithos 2016; 266–267:98–114.

[32] Kaygusuz A, Arslan M, Siebel W, Sipahi F, Ilbeyli N. Geochronological evidence and tectonic significance of Carboniferous magmatism in the southwest Trabzon area, eastern Pontides, Turkey. Int Geol Rev 2012; 54:1776–1800.

[33] Kaygusuz A, Arslan M, Sipahi F, Temizel İ. U–Pb zircon chronology and petrogenesis of

Carboniferous plutons in the northern part of the Eastern Pontides, NE Turkey: Constraints for Paleozoic magmatism and geodynamic evolution. Gondwana Res 2016; 39:327–346.

[34] Kandemir R, Yılmaz C. Lithostratigraphy, facies, and deposition environment of the Lower Jurassic Ammonitico Rosso type sediments (ARTS) in the Gümüşhane area, NE Turkey: Implications for the opening of the northern branch of the Neo-Tethys Ocean. J Asian Earth Sci 2009; 34:586–598.

[35] Saydam Eker Ç, Sipahi F, Kaygusuz A. Trace and rare earth elements as indicators of provenance and depositional environments of Lias cherts in Gumushane, NE Turkey. Geochemistry 2012; 72:167–177.

[36] Gücer MA, Arslan M, Sherlock S, Heaman LM. Permo-Carboniferous granitoids with Jurassic high temperature metamorphism in Central Pontides, Northern Turkey. Mineral Petrol 2016; 110:943–964.

[37] Ağar Ü. Demirözü (Bayburt) ve Köse (Kelkit) bölgesinin jeolojisi. Yayınlanmamış Doktora Tezi 1977.

[38] Dokuz A, Karslı O, Chen B, Uysal I. Sources and petrogenesis of Jurassic granitoids in the Yusufeli area, Northeastern Turkey: Implications for pre- and post-collisional lithospheric thinning of the eastern Pontides. Tectonophysics 2010; 480:259–279.

[39] Eyuboğlu Y, Dudas FO, Santosh M, Zhu DC, Yi K, Chatterjee N, Jeong YJ, Akaryalı E, Liu Z. Cenozoic forearc gabbros from the northern zone of the Eastern Pontides Orogenic Belt, NE Turkey: Implications for slab window magmatism and convergent margin tectonics. Gondwana Res 2016; 33:160–189.

[40] Karslı O, Dokuz A, Kandemir R. Zircon Lu-Hf isotope systematics and U–Pb geochronology, whole-rock Sr-Nd isotopes and geochemistry of the early Jurassic Gokcedere pluton, Sakarya Zone-NE Turkey: a magmatic response to roll-back of the Paleo-Tethyan oceanic lithosphere. Contrib to Mineral Petrol 2017; 172:31.

[41] Pelin S. Alucra (Giresun) Güneydoğu Yöresinin Petrol Olanakları Bakımından Jeolojik İncelenmesi. Karadeniz Tek Üniversitesi Yayınları 1977:87–103.

[42] Aydınçakır E. Subduction-related Late Cretaceous high-K volcanism in the Central Pontides orogenic belt: constraints on geodynamic implications. Geodin Acta 2016; 28:379–411.

[43] Sipahi F, Akpınar İ, Saydam Eker Ç, Kaygusuz A, Vural A, Yılmaz M. Formation of the Eğrikar (Gümüşhane) Fe–Cu skarn type mineralization in NE Turkey: U–Pb zircon age, lithogeochemistry, mineral chemistry, fluid inclusion, and O-H-C-S isotopic compositions. J Geochemical Explor 2017; 182:32–52.

[44] Temizel İ, Arslan M, Yücel C, Yazar Emel A, Kaygusuz A, Aslan Z. U-Pb geochronology, bulk-rock geochemistry and petrology of Late Cretaceous syenitic plutons in the Gölköy (Ordu) area (NE Turkey): Implications for magma generation in a continental arc extension triggered by slab roll-back. J Asian Earth Sci 2019; 171:305–320.

[45] Aydın F, Oğuz Saka S, Şen C, Dokuz A, Aiglsperger T, Uysal İ, Kandemir R, Karslı O, Sarı B, Başer R. Temporal, geochemical and geodynamic evolution of the Late Cretaceous subduction zone volcanism in the eastern Sakarya Zone, NE Turkey: Implications for mantle-crust interaction in an arc setting. J Asian Earth Sci 2020; 192:104217.

[46] Vural A, Kaygusuz A, Akpınar İ. Petrological characteristics of late Cretaceous volcanic rocks of Demirören (Gümüşhane, NE Turkey) region. J Eng Res Appl Sci 2021; 10:1828–1842.

[47] Vural A, Kaygusuz A. Petrographic and geochemical characteristics of late cretaceous volcanic rocks in the vicinity of Avliyana (Gümüşhane, NE Turkey). J Eng Res Appl Sci 2021; 10:1796–1810.

[48] Köprübaşı N, Şen C, Kaygusuz A. Doğu Pontid adayayı granitoyidlerinin karşılaştırılmalı petrografik ve kimyasal özellikleri, KD Türkiye. Uygulamalı Yerbilim Derg 2000; 1:111–120.

[49] Kaygusuz A, Saydam Eker Ç. Geochemical features and petrogenesis of Late Cretaceous subduction-related volcanic rocks in the Değirmentaşı (Torul/Gümüşhane) area, Eastern Pontides (NE Turkey). J Eng Res Appl Sci 2021; 10:1689–1702.

[50] Karslı O, Chen B, Aydın F, Şen C. Geochemical and Sr-Nd-Pb isotopic compositions of the Eocene Dölek and Sariçiçek Plutons, Eastern Turkey: Implications for magma interaction in the genesis of high-K calc-alkaline granitoids in a post-collision extensional setting. Lithos 2007; 98:67–96.

[51] Aydın F, Karslı O, Chen B. Petrogenesis of the Neogene alkaline volcanics with implications for post-collisional lithospheric thinning of the Eastern Pontides, NE Turkey. Lithos 2008; 104:249–266.

[52] Topuz G, Okay AI, Altherr R, Schwarz WH, Siebel W, Zack T, Satir M, Sen C. Post-collisional adakite-like magmatism in the Agvanis Massif and implications for the evolution of the Eocene magmatism in the Eastern Pontides (NE Turkey). Lithos 2011; 125:131–150.

[53] Aydınçakır E. The petrogenesis of Early Eocene non-adakitic volcanism in NE Turkey: Constraints on the geodynamic implications. Lithos 2014; 208:361–377.

[54] Aslan Z, Arslan M, Temizel İ, Kaygusuz A. K-Ar dating, whole-rock and Sr-Nd isotope geochemistry of calc-alkaline volcanic rocks around the Gümüşhane area: Implications for post-collisional volcanism in the Eastern Pontides, Northeast Turkey. Mineral Petrol 2014; 108:245–267.

[55] Eyuboğlu Y, Dudas FO, Thorkelson D, Zhu DC, Liu Z, Chatterjee N, Yi K, Santosh M. Eocene granitoids of northern Turkey: Polybaric magmatism in an evolving arc–slab window system. Gondwana Res 2017; 50:311–345.

[56] Temizel İ, Abdioğlu Yazar E, Arslan M, Kaygusuz A, Aslan Z. Mineral chemistry, whole-rock geochemistry and petrology of Eocene I-type shoshonitic plutons in the Gölköy area (Ordu, NE Turkey). Bull Miner Res Explor 2018; 157:121–152.

[57] Kaygusuz A, Merdan Tutar Z, Yücel C. Mineral chemistry, crystallization conditions and petrography of Cenozoic volcanic rocks in the Bahçecik (Torul/Gumushane) area, Eastern Pontides (NE Turkey). J Eng Res Appl Sci 2017; 6:641–651.

[58] Kaygusuz A, Gucer MA, Yücel C, Aydınçakır E, Sipahi F. Petrography and crystallization conditions of Middle Eocene volcanic rocks in the Aydıntepe-Yazyurdu (Bayburt) area, Eastern Pontides (NE Turkey). J Eng Res Appl Sci 2019; 8:1205–1215.

[59] Temizel İ, Arslan M, Yücel C, Abdioğlu Yazar E, Kaygusuz A, Aslan Z. Eocene tonalite–granodiorite from the Havza (Samsun) area, northern Turkey: adakite-like melts of lithospheric mantle and crust generated in a post-collisional setting. Int Geol Rev 2020; 62:1131–1158.

[60] Yücel C, Arslan M, Temizel İ, Abdioğlu Yazar E, Ruffet G. Evolution of K-rich magmas derived from a net veined lithospheric mantle in an ongoing extensional setting: Geochronology and geochemistry of Eocene and Miocene volcanic rocks from Eastern Pontides (Turkey). Gondwana Res 2017; 45:65–86.

[61] Kaygusuz A, Yücel C, Arslan M, Sipahi F, Temizel İ, Çakmak G, Güloglu ZS. Petrography, mineral chemistry and crystallization conditions of cenozoic plutonic rocks located to the north of Bayburt (Eastern Pontides, Turkey). Bull Miner Res Explor 2018; 157:75–102.

[62] Streckeisen A. To each plutonic rock its proper name. Earth Sci Rev 1976; 12:1–33.

[63] Smith JV, Brown WL. Feldspar Minerals I: Crystal structures, physical, chemical and microtextural properties. Springer Verlage, New York 1988.

[64] Leake EB, Wooley AR, Arps CES, Birch WD, Gilbert MC, Grice JD, Hawthorne FC, Kato A, Kisch HJ, Krivovichev VG, Linthout K, Laird J, et al. Nomenclature of amphiboles report of the subcommittee on amphiboles of the International Mineralogical Association Commission on New Minerals and Mineral Names. Eur J Miner 1997; 9:623–651.

[65] Middlemost EAK. Naming materials in the magma/igneous rock system. Earth Sci Rev 1994; 37:215–224.

[66] Le Maitre RW, Bateman P, Dudek A, Keller J, Lameyre J, Le Bas MJ, Sabine PA, Schmid R, Sorensen H, Streckeisen A, Wooley AR, Zanettin B. A classification of igneous rocks and glossary of terms. Blackwell, Oxford 1989:193 pp.

[67] Chappell BW, White AJR. Two contrasting granite types. Pacific Geol 1974; 8:173–174.

[68] Shand SJ. Eruptive rocks. Their genesis, composition, classification and their relation to ore-deposits. 3rd Ed J Wiley Sons, New York 1947:488 pp.

[69] Pearce JA, Harris NBW, Tindle AG. Trace element discrimination diagram for the tectonic interpretation of granitic rocks. J Petrol 1984; 25:956–983.

[70] Sun SS, McDonough WF. Chemical and isotopic systematics of oceanic basalts: implications for mantle composition and processes. Geol Soc London, Spec Publ 1989; 42:313–345.

[71] Taylor SR, McLennan SM. The Continental Crust; Its Composition and Evolution. Geosci

Text, Blackwell Sci Publ 1985.
[72] Schmidt MW. Amphibole composition in tonalite as a function of pressure: An experimental calibration of the Al-in-hornblende barometer. Contrib to Mineral Petrol 1992; 110:304–310.
[73] Hammarstrom JM, Zen E. Aluminum in hornblende: An empirical igneous geobarometer. Am Mineral 1986; 71:1297–1313.
[74] Hollister LS, Grisson GC, Peters EK, Stowell HH, Sisson VB. Confirmation of the empirical calibration of aluminum in amfibole with pressure of solidification of calc-alkaline plutons. Am Mineral 1987; 34:243–256.
[75] Blundy JD, Holland TJB. Calcic amphibole equilibria and a new amphibole-plagioclase geothermometer. Contrib to Mineral Petrol 1990; 104:208–224.
[76] Watson EB, Harrison TM. Zircon saturation revisited: temperature and composition effects in a variety of crustal magma types. Earth Planet Sci Lett 1983; 64:295–304.
[77] Hanchar JM, Watson EB. Zircon saturation thermometry. Mineral Soc Am Geochemical Soc Am 2003:89–112.
[78] Miller CF, McDowell SM, Mapes RW. Hot and cold granites? Implications of zircon saturation temperatures and preservation of inheritance. Geology 2003; 31:529–532.
[79] White AJR, Chappell BW, Wyborn D. Application of the restite model to the Deddick Granodiorite and its enclaves-A reinterpretation of the observations and data of Maas et al. (1997). J Petrol 1999; 40:413–421.